Anal Bioanal Chem (2007) 389:1869–1878
DOI 10.1007/s00216-007-1568-5

ORIGINAL PAPER

Rapid determination of pK_a values of 20 amino acids by CZE with UV and capacitively coupled contactless conductivity detections

Yveline Henchoz · Julie Schappler · Laurent Geiser · Josiane Prat · Pierre-Alain Carrupt · Jean-Luc Veuthey

Received: 5 June 2007 / Revised: 23 July 2007 / Accepted: 20 August 2007 / Published online: 14 September 2007

Abstract A rapid and universal capillary zone electrophoresis (CZE) method was developed to determine the dissociation constants (pK_a) of the 20 standard proteogenic amino acids. Since some amino acids are poorly detected by UV, capacitively coupled contactless conductivity detection (C^4D) was used as an additional detection mode. The C^4D coupling proved to be very successful on a conventional CE-UV instrument, neither inducing supplementary analyses nor instrument modification. In order to reduce the analysis time for pK_a determination, two strategies were applied: (i) a short-end injection to reduce the effective length, and (ii) a dynamic coating procedure to generate a large electroosmotic flow (EOF), even at pH values as low as 1.5. As a result, the analysis time per amino acid was less than 2 h, using 22 optimized buffers covering a pH range from 1.5 to 12.0 at a constant ionic strength of 50 mM. pK_a values were calculated using an appropriate mathematical model describing the relationship between effective mobility and pH. The obtained pK_a values were in accordance with the literature.

Keywords Amino acids · Capillary zone electrophoresis · Capacitively coupled contactless conductivity detection · Dissociation constants · Dynamic coating

Y. Henchoz · J. Schappler · L. Geiser · J. Prat · J.-L. Veuthey (✉)
Laboratoire de Chimie Analytique Pharmaceutique,
Section des sciences pharmaceutiques, Université de Genève,
Université de Lausanne,
Bd d'Yvoy 20,
1211 Geneva 4, Switzerland
e-mail: jean-luc.veuthey@pharm.unige.ch

Y. Henchoz · P.-A. Carrupt
Unité de Pharmacochimie, Section des sciences pharmaceutiques,
Université de Genève, Université de Lausanne,
Quai Ernest Ansermet 30,
1211 Geneva 4, Switzerland

Abbreviations

ADME	Absorption, distribution, metabolism and excretion
BGE	Background electrolyte
C^4D	Capacitively coupled contactless conductivity detection
CE	Capillary electrophoresis
CZE	Capillary zone electrophoresis
EOF	Electroosmotic flow
FS	Fused silica
ID	Internal diameter
NCE	New chemical entity

Introduction

Evaluating physicochemical properties of new chemical entities (NCEs) at an early stage of drug development is mandatory to reduce attrition rates due to poor biopharmaceutical properties. Among these properties, ionisation constants (pK_a) are needed to predict ADME (absorption, distribution, metabolism and excretion) behaviour, in particular to understand pH-related permeation mechanisms and solubility characteristics. Traditionally, potentiometric and spectrophotometric methods have been used to determine pK_a values [1]. In the last 15 years, capillary zone electrophoresis (CZE) with UV detection confirmed its potential for measuring pK_a values in a simple automated way [2–6]. Moreover, this technique consumes minor amounts of sample, is compatible with samples of low purity and is cost effective.

Within recent years, in addition to UV detection, conductivity and particularly capacitively coupled contactless conductivity detection (C^4D) have become frequently used with CE [7–9]. The miniaturized dimensions of this

detector and its simplicity have induced great interest, and devices are now commercially available permitting one to achieve good sensitivity and robustness. CE-C^4D is suitable for measuring small inorganic and organic ions [10], and is particularly well adapted for chromophore- and fluorophore-free compounds. Generally, indirect UV detection strategies are used for non-UV absorbing analytes, but they present a lack of sensitivity. Furthermore, the strong UV-absorbing agent added to the background electrolytes (BGEs) must possess an electrophoretic mobility similar to the analytes to avoid important electrodispersion phenomena. In contrast, C^4D is a reliable detection whatever the type of BGEs or analytes.

Thereby, it emerges as a near-universal detector, particularly well adapted to CE for determining physicochemical parameters, since such methods involve the use of specific conditions in regards to ionic strength and pH. Implementation of C^4D over other detection techniques is not skill-demanding in the case of pure solute analysis, and commercially available instruments are easily hyphenated to CE. Features include on-capillary detection, great flexibility in capillary handling, capillary material independence and contactless detection. The last of these features allows the application of high separation voltage without interferences with the detection signal. Moreover, the detector can be freely positioned along the capillary and may therefore be placed where the apparent selectivity is optimum. Other advantages include providing a convenient second point of detection in addition to photometric detection, positioning several C^4D cells along the capillary simultaneously and implementing in microchip and array technologies [11].

CZE is well suited for the separation of amino acids and peptides [12]. The pK_a values of the 20 most common amino acids which do not possess an ionisable function on their lateral chain were determined with a conventional CZE method but required long analysis times especially at low pH (more than 30 min per analysis) [13]. More recently, Gaš and co-workers determined pK_a values of the carboxylic groups of these amino acids with conductivity detection using two conductivity cells which enabled one to reduce the effective length at low pH and thus the analysis time (less than 15 min per analysis) [14, 15].

In order to reduce the analysis time for pK_a determination, different generic strategies have been reported, such as pressure-assisted capillary electrophoresis [16–19], short-end injection [20, 21], multiplexed capillary electrophoresis [22] or dynamic coated capillaries [23]. It can be noted that short-end injection and especially pressure-assisted strategies reduce apparent peak efficiency, which can decrease precision of migration time determination. All these approaches were generally used separately, whereas some of them may be combined for further time saving.

The aim of the present work consisted in developing a rapid and near-universal CZE method using short-end injection combined with a dynamic coating procedure for determining pK_a values of ionisable functions of 20 natural amino acids. C^4D was used in combination with UV to detect poorly UV absorbing compounds in the same run without instrument modification.

Theory

The *i*th dissociation of a fully protonated polyprotic solute H_nX^z is described as follow:

$$H_{n-i+1}X^{z-i+1} \rightleftharpoons H_{n-i}X^{z-i} + H^+ \quad (1)$$

where n is the total number of ionisable groups and z the charge of the fully protonated species. For measurements performed in non-ideal solutions, the thermodynamic dissociation constant of the *i*th dissociation step is defined as:

$$K_{ai}(\text{thermodynamic}) = \frac{[H_{n-i}X^{z-i}]}{[H_{n-i+1}X^{z-i+1}]} \cdot \frac{\gamma^{z-i}}{\gamma^{z-i+1}} \cdot a_{H^+} \quad (2)$$

where a_{H^+} is the proton activity, terms in brackets represent molar concentrations of the electrical species of the solute and γ terms are the activity coefficients of charged species other than proton. The measurements giving apparent dissociation constants directly related to experimental conditions, the determination of thermodynamic constants is only indirectly possible using the estimation of γ terms by Eq. (3). Indeed, activity coefficients can be estimated by the Davies equation [24] extended from the Debye–Hückel model to take into account the effect of ionic strength (I) upon dissociation equilibria. According to IUPAC guidelines, the semi-empirical Davies equation (Eq. (3)) can be used for univalent and multivalent ions up to I=0.2 M [25]:

$$\log \gamma = -A \cdot z^2 \left(\frac{\sqrt{I}}{1+\sqrt{I}} - C \cdot I \right) \quad (3)$$

where A=0.509 and C=0.3 in aqueous solutions at 25 °C. The Davies equation can also be used to compare measurements performed under different experimental conditions, for example at different ionic strengths. For simplification reasons, the notation K_a used in this paper will refer to apparent dissociation constants measured under different conditions.

The effective mobility (μ_{eff}) of a polyprotic compound H_nX^z, coexisting in different ionised states at a given pH,

depends on the molar fraction (χ_j) and on the effective mobility of each individual species :

$$\mu_{\text{eff}} = \sum_{i=0}^{n} \chi_{\text{H}_{n-i}\text{X}^{z-i}} \cdot \mu_{\text{H}_{n-i}\text{X}^{z-i}} \tag{4}$$

Therefore,

$$\mu_{\text{eff}} = \sum_{i=0}^{n} \frac{[\text{H}_{n-i}\text{X}^{z-i}]}{\sum_{i=0}^{n} [\text{H}_{n-i}\text{X}^{z-i}]} \cdot \mu_{\text{H}_{n-i}\text{X}^{z-i}} \tag{5}$$

Using Eq. (2), the previous expression can be rewritten as:

$$\mu_{\text{eff}} = \sum_{i=0}^{n} \frac{\left[\prod_{j=1}^{i} K_{\text{a}j}\right] \cdot a_{\text{H}^+}^{n-i}}{\sum_{i=0}^{n} \left[\prod_{j=1}^{i} K_{\text{a}j}\right] \cdot a_{\text{H}^+}^{n-i}} \cdot \mu_{\text{H}_{n-i}\text{X}^{z-i}} \tag{6}$$

Considering $K_{\text{a}j} = 10^{-\text{p}K_{\text{a}j}}$ and $a_{\text{H}^+}^{n} = 10^{-n\text{pH}}$ Eq. (6) can be rearranged as a function of pH and p$K_{\text{a}j}$:

$$\mu_{\text{eff}} = \sum_{i=0}^{n} \frac{\left[\prod_{j=1}^{i} 10^{-\text{p}K_{\text{a}j}}\right] \cdot 10^{(i-n)\text{pH}}}{\sum_{i=0}^{n} \left[\prod_{j=1}^{i} 10^{-\text{p}K_{\text{a}j}}\right] \cdot 10^{(i-n)\text{pH}}} \cdot \mu_{\text{H}_{n-i}\text{X}^{z-i}} \tag{7}$$

This equation allows the determination of pK_{a} values from a plot of μ_{eff} as a function of pH. It can be applied to different ionisable compounds as shown in the Appendix.

Practically, μ_{eff} of an analyte can be measured as:

$$\mu_{\text{eff}} = \frac{L_{\text{eff}} \cdot L_{\text{tot}}}{U} \cdot \left(\frac{1}{t_{\text{m}}} - \frac{1}{t_{\text{EOF}}}\right) \tag{8}$$

where t_{m} and t_{EOF} are the migration times (s) of the analyte and the neutral marker, respectively, U is the applied voltage (V), L_{tot} the total capillary length (cm) and L_{eff} the effective capillary length (cm).

Materials and methods

Chemicals

L-Alanine, L-asparagine, L-aspartic acid, L-cysteine, L-glutamic acid, L-glutamine, L-methionine, L-proline, L-serine, L-threonine, L-tryptophan, L-valine, L-arginine, L-histidine, L-isoleucine, L-leucine, L-lysine, L-phenylalanine and L-tyrosine were purchased from Fluka (Buchs, Switzerland). L-Glycine was obtained from Merck (Dietikon, Switzerland).

Phosphoric acid (H_3PO_4), formic acid (HCOOH), acetic acid (CH_3COOH), MES (2-(*N*-morpholino)ethanesulfonic acid), MOPS (3-morpholinopropanesulfonic acid), TRICINE (*N*-(tris(hydroxymethyl)-methyl)glycine) and CHES (2-(cyclohexylamino)ethanesulfonic acid) were purchased from Fluka (Buchs, Switzerland). HPLC grade methanol was supplied by Romil (Kölliken, Switzerland), analytical reagent grade acetone by Acros Organics (Basel, Switzerland), hydrochloric acid by Riedel-de-Haën (Buchs, Switzerland) and 1 M Titrinorm sodium hydroxide by VWR (Dietikon, Switzerland). The Ceofix® pH 2.5 solutions were obtained from Analis (Namur, Belgium). All solutions were prepared using ultra-pure water supplied by a Milli-Q Waters Purification System from Millipore (Bedford, MA, USA).

Buffers and samples preparation

Twenty seven buffers covering a pH range from 1.5 to 12.0 were prepared. They were set at a constant ionic strength of 50 mM, and are listed exhaustively in Table 1. The pH values were measured with a Mettler-Toledo SevenMulti pH meter (Schwerzenbach, Switzerland), calibrated daily with four aqueous solutions at pH 2.00, 4.00, 7.00 and 10.00 from Riedel-de-Haën (Buchs, Switzerland). Stock solutions of each amino acid were prepared at a concentration of 1 mg mL^{-1}. Samples were set at a concentration of 0.1 mg mL^{-1} in BGE, water and acetone (EOF neutral marker) 85:10:5 (V:V:V).

Instrumentation

CE experiments were performed with an HP^{3D}CE system (Agilent, Waldbronn, Germany) equipped with an on-capillary diode array detector (8.5 cm from the anode), an on-capillary capacitively coupled contactless conductivity detector (13.65 cm from the anode), an autosampler and a power supply able to deliver up to 30 kV. UV detection was carried out at 195 nm for amino acids and 260 nm for acetone. C^{4}D was performed with a TraceDec detector (Innovative Sensor Technologies GmbH, Strasshof, Austria). The conductivity sensor consisted of two electrodes separated by a detection gap of 1 mm, housed inside an aluminium case and positioned along the capillary by sliding it into the desired position. CE ChemStation (Agilent) was used for CE and UV control, data acquisition and data handling. C^{4}D was set at a frequency of 300 kHz and an amplitude of 100 V for the AC signal. C^{4}D Tracemon (Istech), version 0.07a, was used for conductivity detector control. Analyses were performed in uncoated fused silica (FS) capillaries (BGB Analytik AG, Böckten, Switzerland) with 50-μm inner diameter (ID) and 32.5-cm total length.

Table 1 Preparation of buffers at 50 mM ionic strength and applied voltages

Buffering species (mM)	NaOH (mM)	Theoretical pH (at 25 °C)	Measured pH (at 25 °C)	Buffer capacity (mM/pH unity)	Applied voltage (kV)
H_3PO_4 220.5	11.0	1.5	1.495	178.6	3.5
H_3PO_4 103.9	37.7	2.0	1.988	89.3	5.0
H_3PO_4 67.0	46.1	2.5	2.502	38.4	6.0
HCOOH 278.9	48.8	3.0	2.965	105.1	6.0
HCOOH 122.4	49.6	3.5	3.483	72.7	6.5
HCOOH 72.9	49.9	4.0	4.009	37.3	6.5
CH_3COOH 123.0	50.0	4.5	4.500	72.3	8.0
CH_3COOH 73.1	50.0	5.0	4.992	37.3	8.0
CH_3COOH 57.3	50.0	5.5	5.461	14.7	8.0
MES 104.7	50.0	6.0	5.991	63.0	8.0
MES 67.3	50.0	6.5	6.423	30.1	8.0
MOPS 114.0	50.0	7.0	6.978	39.3	8.0
MOPS 70.2	50.0	7.5	7.470	15.8	8.0
MOPS 56.4	50.0	8.0	7.934	5.4	8.0
Tricine 68.1	50.0	8.5	8.472	31.1	8.0
Tricine 55.7	50.0	9.0	8.928	11.8	8.0
CHES 75.4	50.0	9.5	9.613	53.6	8.0
CHES 57.9	49.9	10.0	10.077	24.0	8.0
CHES 52.1	49.6	10.5	10.480	9.5	8.0
H_3PO_4 14.7	32.2	11.0	11.072	6.4	8.0
H_3PO_4 12.0	31.3	11.5	11.527	15.5	8.0
H_3PO_4 8.1	33.0	12.0	11.962	35.4	6.0

Samples were kept at room temperature in the autosampler and introduced by short-end injection, i.e. the polarity was reversed and samples were injected at the detector side. An injection equivalent to 0.4 % of the capillary's total length was performed by applying a pressure of 48 mbar s (12 mbar for 4 s). During analysis, a voltage of 3.5 to 8 kV (depending on the running buffer) was applied to avoid the detrimental effect of Joule heating. The capillary was thermostated at 25 °C by a high velocity air stream. Before its first use, the capillary was sequentially rinsed (1 bar) with methanol, 1 M HCl, water, 1 M NaOH, 0.1 M NaOH and water (5 min each). Between different pH buffers, several washing steps (1 bar) were employed, namely water (1 min), Ceofix® initiator (0.5 min), Ceofix® accelerator (1 min), BGE (5 min) and pre-electrophoresis (3.5–8 kV, 5 min). Between analyses, the capillary was rinsed (1 bar) with BGE for 1 min. When not in use, the capillary was rinsed with water and dry stored.

Procedure

Each compound was injected once at each pH. The effective mobility was calculated from analyte and neutral marker migration times (Eq. (8)). Calculated effective mobilities were reported as a function of pH, giving rise to sigmoidal curves. With a GraphPad Prism 4.02 software (GraphPad Software, San Diego, CA, USA), non-linear regressions were performed to determine apparent pK_a values at I=50 mM, using the appropriate equation described in the Appendix.

Results and discussion

Previously, pK_a values of more than ten drugs were determined by CZE-UV with a dynamic coating of the capillary to ensure high EOF, whatever the buffer pH [23]. In the present work, this procedure was combined with short-end injection to further increase the throughput and C^4D was used as an additional detector for poorly UV absorbing compounds.

Analytical development

Twenty-two buffers reported in Table 1 were selected for pK_a determination, which covered a pH range from 1.5 to 12.0 with an increment of 0.5 pH units between each. A constant ionic strength was used to avoid μ_{eff} variations [26–28] and keep activity coefficients constant (Eq. (3)). The ionic strength was set at 50 mM as a compromise between sufficient buffer capacity and low Joule heating.

The nature of the buffers was carefully selected to insure the best buffer capacity as well as minimal interactions with analytes. As shown in Fig. 1, μ_{eff} values of arginine and lysine were lower with phosphate rather than MES or

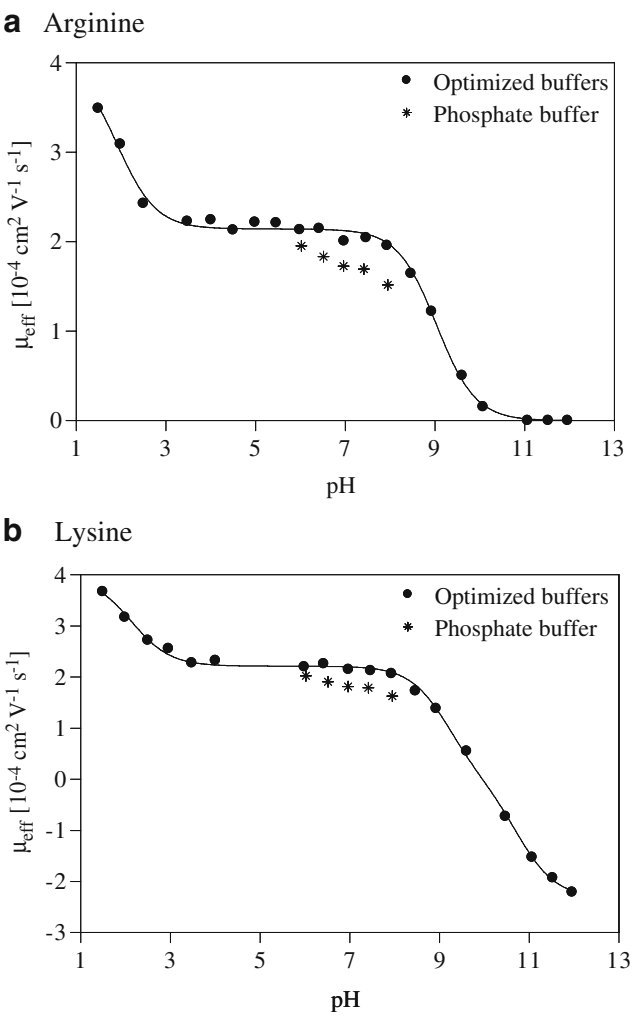

Fig. 1 Comparison of the relationship between μ_{eff} and pH for arginine (**a**) and lysine (**b**) by CZE-UV: phosphate buffers (*) vs. optimized buffers (•)

MOPS buffers from pH 6.0 to 8.0. At these pH values, these amino acids were mainly present in their monoanionic dicationic form and may thus be associated by electrostatic interactions with monohydrogenophosphate ions. As expected from theory, this phenomenon increased with pH values, since the concentration of monohydrogenophosphate ions also increased. These interactions were more important with amino acids possessing a positively charged lateral chain, such as arginine and lysine. As a consequence, MES and MOPS buffers were preferred to phosphate buffers in this pH range. Moreover, those buffers are more appropriate to CZE-C^4D, since amphoteric electrolytes with a low equivalent conductivity at considerably high concentrations can limit peak dispersion effects.

The applied voltage was adjusted to the buffer conductivity to prevent excessive Joule heating. For this purpose, the voltage was adapted to remain in the linearity domain of Ohm's law. As a result, voltages between 3.5 and 8.0 kV were applied, depending on the buffer (Table 1). The lowest voltages were applied with extremely acidic or basic buffers, because of their high conductivities.

Samples were diluted in 85% running BGE to avoid seriously distorted triangular peak shapes which induced inaccurate determination of migration times. Such distorted peaks are due to electrodispersion phenomena which are quite pronounced for amino acids possessing very high diffusion coefficients. Low differences in conductivity and pH between the running buffer and the sample zone limited electrodispersion [29, 30]. Therefore, peak shapes were symmetrical, allowing the precise determination of migration times. However, this procedure was at the expense of C^4D sensitivity, since maximal sensitivity should be obtained when the highest possible conductivity difference between the analyte zone and BGE is achieved. Furthermore, matching sample and BGE global conductivity led to poor sample stacking, which was also detrimental to sensitivity [9, 30].

Curves of μ_{eff} as a function of pH were determined with UV and C^4D detections. Both detection methods complemented each other since some amino acids were not determined by UV because of their lack of chromophore, but were easily detected by C^4D. For instance, glycine, lysine and glutamic acid were hardly achieved by UV, while C^4D provided large peaks as shown in Fig. 2. Likewise, other amino acids were better detected by C^4D than UV: alanine, aspartic acid, isoleucine, leucine, proline, serine, threonine, valine. In contrast, some amino acids were better detected by UV, but scarcely by C^4D due to similar conductivity with the BGE. Although some amino acids were poorly detected by one of the two used detectors, it is noteworthy that in all cases enough points were achieved to determine pK_a values by UV as well as C^4D. Therefore, the combination of both detectors proved to be very useful, and allowed the analysis of the 20 amino acids in the 22 used buffers.

Since the main objective of this study was to reduce the analysis time, a dynamic coating procedure was combined with a short-end injection. The dynamic coating procedure generated a large EOF (ca. 5×10^{-4} cm^2 V^{-1} s^{-1}) whatever the buffer with pH values as low as 1.5. Moreover, it prevented intrusive interactions between compounds and capillary walls [12]. Concerning the short-end injection, this approach reduced the analysis time drastically without enhancing Joule heating by shortening the capillary total length. As a result, the total analysis time (i.e. in the 22 buffers) took less than 2 h per compound, including the washing steps, injection, vial permutation and separation times.

pK_a determination

Plots of μ_{eff} as a function of pH are shown in Fig. 3 for selected proteogenic amino acids. At any pH, μ_{eff} of a given

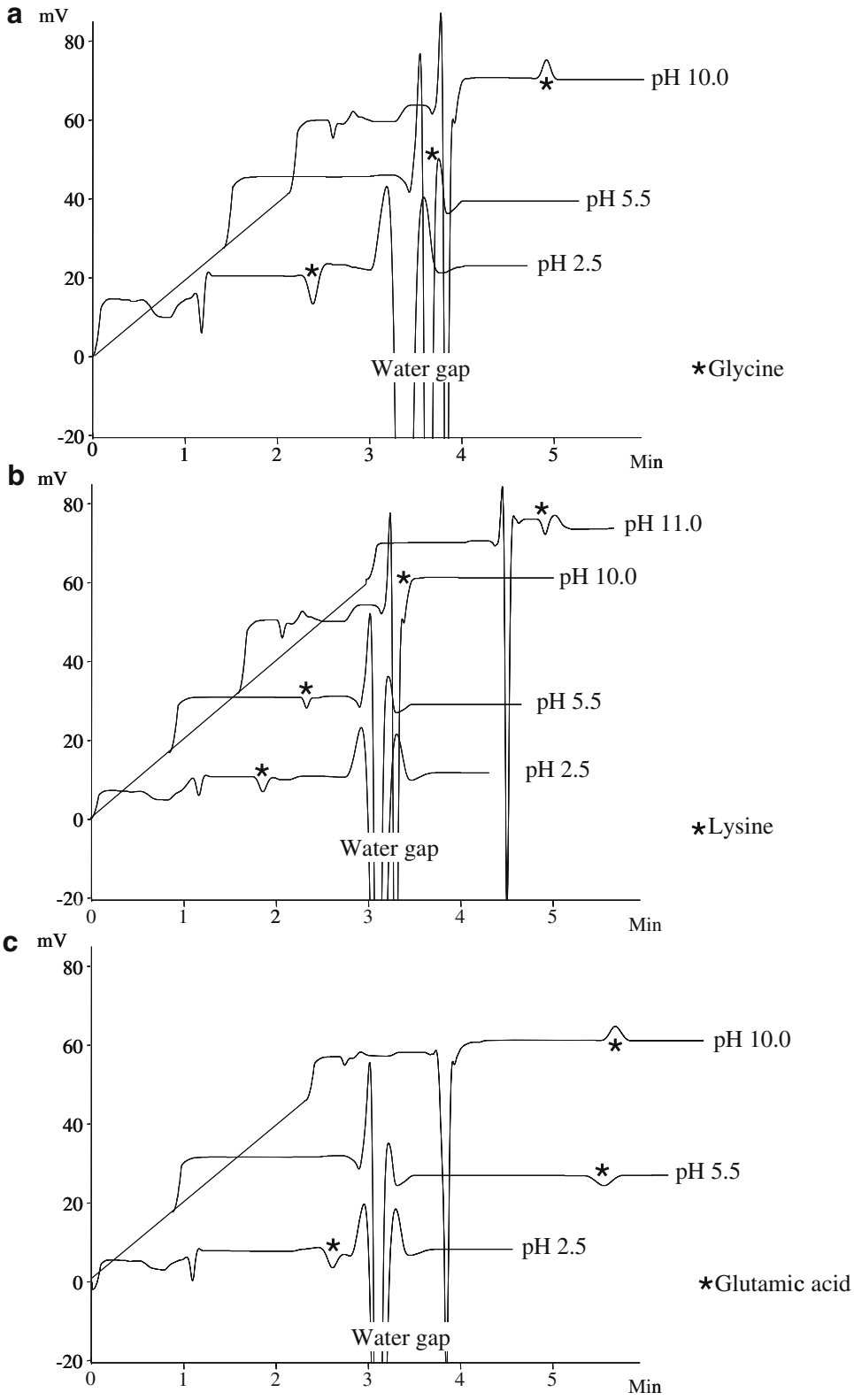

Fig. 2 **a** CE-C^4D analysis of glycine at pH 2.5, 5.5 and 10.0. **b** CE-C^4D analysis of glycine at pH 2.5, 5.5, 10.0 and 11.0. **c** CE-C^4D analysis of glutamic acid at pH 2.5, 5.5 and 10.0. BGE and separation voltage: as described in Table 1, capillary dimensions 50-μm ID x 32.5 cm, effective length 13.65 cm, injection 48 mbar s, temperature 25 °C

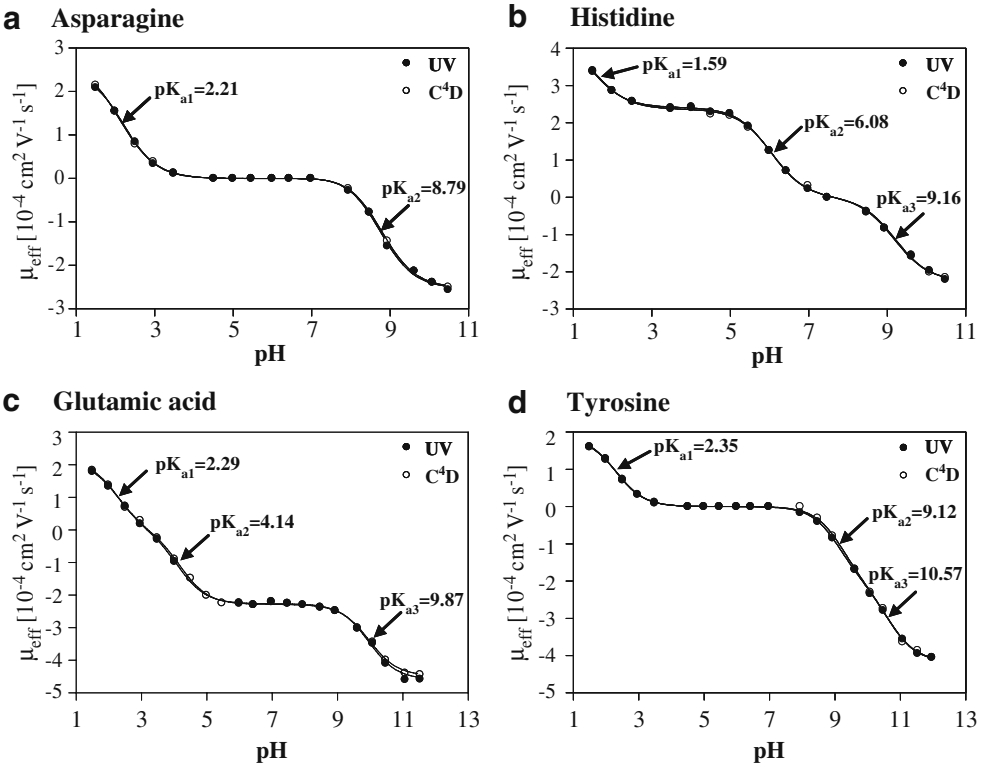

Fig. 3 Relationship between μ_{eff} and pH for **a** monoacidic monobasic amino acid asparagine, **b** monoacidic dibasic amino acid histidine, **c** diacidic monobasic amino acid glutamic acid and **d** tyrosine

Table 2 Apparent pK_a values at 150 mM ionic strength and 25 °C

Amino acid	C-terminal		N-terminal		Side-chain	
	UV	C^4D	UV	C^4D	UV	C^4D
Alanine	2.35±0.12	2.39±0.08	9.83±0.15	9.82±0.10		
Arginine	1.98±0.23	1.95±0.22	9.00±0.08	9.04±0.08	>12	>12
Asparagine	2.23±0.17	2.18±0.11	8.77±0.06	8.80±0.04		
Aspartic acid	2.02±0.14	1.99±0.08	10.03±0.15	10.01±0.09	3.66±0.12	3.73±0.07
Cysteine	2.05±0.10	2.04±0.08	10.26±0.50	10.19±0.45	8.44±0.12	8.42±0.11
Glutamine	2.21±0.15	2.24±0.11	9.07±0.02	9.16±0.06		
Glutamic acid	2.29±0.16	2.29±0.11	9.87±0.13	9.87±0.08	4.10±0.09	4.17±0.06
Glycine	2.43±0.10	2.43±0.08	9.60±0.08	9.65±0.08		
Histidine	1.54±0.70	1.64±0.45	9.18±0.08	9.14±0.08	6.07±0.05	6.09±0.06
Isoleucine	2.36±0.07	2.39±0.07	9.61±0.06	9.67±0.08		
Leucine	2.37±0.06	2.43±0.05	9.62±0.06	9.71±0.07		
Lysine	2.21±0.23	2.28±0.22	9.19±0.10	9.23±0.09	10.75±0.13	10.70±0.13
Methionine	2.19±0.12	2.26±0.10	9.14±0.04	9.17±0.04		
Phenylalanine	2.18±0.12	2.21±0.15	9.15±0.04	9.17±0.06		
Proline	1.99±0.13	2.03±0.16	10.81±0.08	10.77±0.10		
Serine	2.16±0.18	2.24±0.11	9.09±0.04	9.15±0.05		
Threonine	2.27±0.21	2.28±0.13	8.98±0.04	9.03±0.04		
Tryptophan	2.41±0.10	2.46±0.12	9.40±0.03	9.43±0.10		
Tyrosine	2.33±0.07	2.36±0.10	9.09±0.10	9.15±0.12	10.57±0.11	10.56±0.15
Valine	2.46±0.15	2.42±0.15	9.67±0.07	9.63±0.08		

Values are reported as mean ± 95% confidence interval and were converted to 150 mM physiological ionic strength by Eqs. (2) and (3). The activity correction is ± 0.03 for monocharged species and ± 0.10 for dicharged species

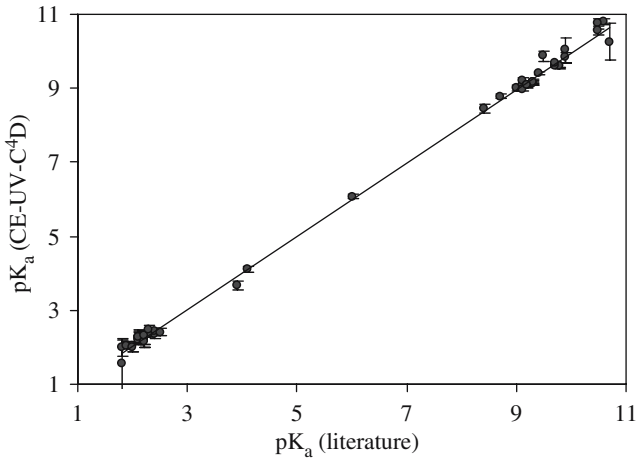

Fig. 4 Plot of experimental pK_a values obtained by CE-UV with 95% confidence interval (Table 2) vs. pK_a values from literature [31]. Slope (CI) 0.988 (0.976 to 1.003), intercept (CI) 0.069 (−0.004 to 0.133)

compound depends on the molar fraction of each ionised form (Eq.(4)). For example, asparagine (Fig. 3a) is a typical amino acid possessing two pK_a values, showing a first inflection point between pH 1.5 and 3.5 (pK_a=2.21) and a second inflection point between pH 7.5 and 10.5 (pK_a= 8.79). Twelve other amino acids also possess two pK_a values, and present the same relationship between μ_{eff} and pH. The curves of the seven other amino acids exhibited three inflection points corresponding to three dissociation constants as is the case for the monoacidic dibasic amino acid histidine (Fig. 3b) and the diacidic monobasic amino acid glutamic acid (Fig. 3c). In a few cases, dissociation steps partially overlapped due to close pK_a values.

The pK_a values of the 20 investigated amino acids were determined using the appropriate fitting model (Appendix). pK_a values of carboxylic and amino groups as well as pK_a values of lateral chains were obtained for the first time by CE. The ionisation constant was affected by the ionic strength as demonstrated by Eq. (3). It was then necessary to report the ionic strength as well as temperature, since ionisation constants are also temperature-dependent. Since most of the results reported in the literature are determined at a physiological ionic strength of 150 mM [31], the obtained apparent pK_a values at 50 mM ionic strength were converted to 150 mM ionic strength using Eq. (3) and data are listed in Table 2.

With this procedure, 95% confidence intervals were typically lower than 0.20 units. They were higher at the limits of the investigated pH range (1.5 to 12.0). For instance, the pK_a of arginine lateral chain (>12) was outside the pH range used in this study and therefore was not determined. The 95% confidence intervals were also high for overlapping pK_a values as for example pK_{a2} and pK_{a3} of tyrosine (Fig. 3d), lysine, aspartic acid and cysteine. pK_a values obtained by UV detection and C^{4}D were similar; by taking into account the 95% confidence interval, they were considered identical.

As a comparison, pK_a values of the 20 amino acids were plotted versus literature pK_a values obtained at 25 °C (Fig. 4) [32]. The CZE-measured pK_a values are correlated with those reported in the literature by using Passing–Bablok regression [33, 34]. Considering the 95% confidence interval, the slope of the linear regression was equal to 1 and the *y*-intercept 0. The CZE-measured pK_a values could thus be considered similar to the literature values.

Conclusion

A rapid and universal CZE-UV-C^{4}D method was developed, using 22 optimal background electrolytes, to determine pK_a values of all ionisable functions of 20 amino acids. Two generic strategies, namely short-end injection and dynamic coated capillaries, allowed the successful determination of all pK_a values in less than 2 h per compound. The combined use of both detectors extended the method to poorly UV absorbing amino acids without supplementary analyses. This powerful combination allows the application of this method to the determination of pK_a values for almost any kind of solute.

Importantly, this methodology can be transferred to array systems in order to perform several analyses simultaneously as C^{4}D might be compatible with such instruments. To further increase throughput, a mass spectrometer could also be hyphenated to CE which would allow a greater pooling of compounds per analysis owing to the additional selectivity offered by MS [35].

Appendix

Table 3 Model equations for pK_a determination by CZE

Ionisable compounds	Parameters	Model equation according to Eq. (7)
monoacid	n = 1 z = 0	$\mu_{eff} = \frac{\mu_{X^-} 10^{-pK_{a1}}}{10^{-pH} + 10^{-pK_{a1}}}$
monobase	n = 1 z = 1	$\mu_{eff} = \frac{\mu_{HX^+} 10^{-pH}}{10^{-pH} + 10^{-pK_{a1}}}$
diacid	n = 2 z = 0	$\mu_{eff} = \frac{\mu_{HX^-} 10^{-pK_{a1}-pH} + \mu_{X^{2-}} 10^{-pK_{a2}-pK_{a1}}}{10^{-2pH} + 10^{-pK_{a1}-pH} + 10^{-pK_{a2}-pK_{a1}}}$
monoacidic monobasic ampholyte	n = 2 z = 1	$\mu_{eff} = \frac{\mu_{H_2X^+} 10^{-2pH} + \mu_{X^-} 10^{-pK_{a2}-pK_{a1}}}{10^{-2pH} + 10^{-pK_{a1}-pH} + 10^{-pK_{a2}-pK_{a1}}}$
dibase	n = 2 z = 2	$\mu_{eff} = \frac{\mu_{H_2X^{2+}} 10^{-2pH} + \mu_{HX^+} 10^{-pK_{a1}-pH}}{10^{-2pH} + 10^{-pK_{a1}-pH} + 10^{-pK_{a2}-pK_{a1}}}$
triacid	n = 3 z = 0	$\mu_{eff} = \frac{\mu_{H_2X^-} 10^{-pK_{a1}-2pH} + \mu_{HX^{2-}} 10^{-pK_{a2}-pK_{a1}-pH} + \mu_{X^{3-}} 10^{-pK_{a3}-pK_{a2}-pK_{a1}}}{10^{-3pH} + 10^{-pK_{a1}-2pH} + 10^{-pK_{a2}-pK_{a1}-pH} + 10^{-pK_{a3}-pK_{a2}-pK_{a1}}}$
diacidic monobasic ampholyte	n = 3 z = 1	$\mu_{eff} = \frac{\mu_{H_3X^+} 10^{-3pH} + \mu_{HX^-} 10^{-pK_{a2}-pK_{a1}-pH} + \mu_{X^{2-}} 10^{-pK_{a3}-pK_{a2}-pK_{a1}}}{10^{-3pH} + 10^{-pK_{a1}-2pH} + 10^{-pK_{a2}-pK_{a1}-pH} + 10^{-pK_{a3}-pK_{a2}-pK_{a1}}}$
monoacidic dibasic ampholyte	n = 3 z = 2	$\mu_{eff} = \frac{\mu_{H_3X^{2+}} 10^{-3pH} + \mu_{H_2X^+} 10^{-pK_{a1}-2pH} + \mu_{X^-} 10^{-pK_{a3}-pK_{a2}-pK_{a1}}}{10^{-3pH} + 10^{-pK_{a1}-2pH} + 10^{-pK_{a2}-pK_{a1}-pH} + 10^{-pK_{a3}-pK_{a2}-pK_{a1}}}$
tribase	n = 3 z = 3	$\mu_{eff} = \frac{\mu_{H_3X^{3+}} 10^{-3pH} + \mu_{H_2X^{2+}} 10^{-pK_{a1}-2pH} + \mu_{HX^+} 10^{-pK_{a2}-pK_{a1}-pH}}{10^{-3pH} + 10^{-pK_{a1}-2pH} + 10^{-pK_{a2}-pK_{a1}-pH} + 10^{-pK_{a3}-pK_{a2}-pK_{a1}}}$
tetracid	n = 4 z = 0	$\mu_{eff} = \frac{\mu_{H_3X^-} 10^{-pK_{a1}-3pH} + \mu_{H_2X^{2-}} 10^{-pK_{a2}-pK_{a1}-2pH} + \mu_{HX^{3-}} 10^{-pK_{a3}-pK_{a2}-pK_{a1}-pH} + \mu_{X^{4-}} 10^{-pK_{a4}-pK_{a3}-pK_{a2}-pK_{a1}}}{10^{-4pH} + 10^{-pK_{a1}-3pH} + 10^{-pK_{a2}-pK_{a1}-2pH} + 10^{-pK_{a3}-pK_{a2}-pK_{a1}-pH} + 10^{-pK_{a4}-pK_{a3}-pK_{a2}-pK_{a1}}}$
triacidic monobasic ampholyte	n = 4 z = 1	$\mu_{eff} = \frac{\mu_{H_4X^+} 10^{-4pH} + \mu_{H_2X^-} 10^{-pK_{a2}-pK_{a1}-2pH} + \mu_{HX^{2-}} 10^{-pK_{a3}-pK_{a2}-pK_{a1}-pH} + \mu_{X^{3-}} 10^{-pK_{a4}-pK_{a3}-pK_{a2}-pK_{a1}}}{10^{-4pH} + 10^{-pK_{a1}-3pH} + 10^{-pK_{a2}-pK_{a1}-2pH} + 1\,0^{-pK_{a3}-pK_{a2}-pK_{a1}-pH} + 10^{-pK_{a4}-pK_{a3}-pK_{a2}-pK_{a1}}}$
diacidic dibasic ampholyte	n = 4 z = 2	$\mu_{eff} = \frac{\mu_{H_4X^{2+}} 10^{-4pH} + \mu_{H_3X^+} 10^{-pK_{a1}-3pH} + \mu_{HX^-} 10^{-pK_{a3}-pK_{a2}-pK_{a1}-pH} + \mu_{X^{2-}} 10^{-pK_{a4}-pK_{a3}-pK_{a2}-pK_{a1}}}{10^{-4pH} + 10^{-pK_{a1}-3pH} + 10^{-pK_{a2}-pK_{a1}-2pH} + 10^{-pK_{a3}-pK_{a2}-pK_{a1}-pH} + 10^{-pK_{a4}-pK_{a3}-pK_{a2}-pK_{a1}}}$
monoacidic tribasic ampholyte	n = 4 z = 3	$\mu_{eff} = \frac{\mu_{H_4X^{3+}} 10^{-4pH} + \mu_{H_3X^{2+}} 10^{-pK_{a1}-3pH} + \mu_{H_2X^+} 10^{-pK_{a2}-pK_{a1}-2pH} + \mu_{X^-} 10^{-pK_{a4}-pK_{a3}-pK_{a2}-pK_{a1}}}{10^{-4pH} + 10^{-pK_{a1}-3pH} + 10^{-pK_{a2}-pK_{a1}-2pH} + 10^{-pK_{a3}-pK_{a2}-pK_{a1}-pH} + 10^{-pK_{a4}-pK_{a3}-pK_{a2}-pK_{a1}}}$
tetrabase	n = 4 z = 4	$\mu_{eff} = \frac{\mu_{H_4X^{4+}} 10^{-4pH} + \mu_{H_3X^{3+}} 10^{-pK_{a1}-3pH} + \mu_{H_2X^{2+}} 10^{-pK_{a2}-pK_{a1}-2pH} + \mu_{HX^+} 10^{-pK_{a3}-pK_{a2}-pK_{a1}-pH}}{10^{-4pH} + 10^{-pK_{a1}-3pH} + 10^{-pK_{a2}-pK_{a1}-2pH} + 10^{-pK_{a3}-pK_{a2}-pK_{a1}-pH} + 10^{-pK_{a4}-pK_{a3}-pK_{a2}-pK_{a1}}}$

References

1. Poole SK, Patel S, Dehring K, Workman H, Poole CF (2004) J Chromatogr 1037:445–454
2. Uhrova M, Miksik I, Deyl Z, Bellini S (1997) Proc Control Qual 10:151–167
3. Kerns EH (2001) J Pharm Sci 90:1838–1858
4. Jia Z (2005) Curr Pharm Anal 1:41–56
5. Wan H, Thompson RA (2005) Drug Discov Today 2:171–178
6. Wan H, Ulander J (2006) Expert Opin Drug Metab Toxicol 2:139–155
7. Kuban P, Hauser PC (2004) Electroanalysis 16:2009–2021
8. Guijt RM, Evenhuis CJ, Macka M, Haddad PR (2004) Electrophoresis 25:4032–4057
9. Zemann AJ (2003) Electrophoresis 24:2125–2137
10. Solinova V, Kasicka V (2006) J Sep Sci 29:1743–1762
11. Macka M, Hutchinson J, Zemann A, Shusheng Z, Haddad PR (2003) Electrophoresis 24:2144–2149
12. Kasicka V (2003) Electrophoresis 24:4013–4046
13. Yang L, Yuan Z (1999) Electrophoresis 20:2877–2883
14. Vcelakova K, Zuskova I, Kenndler E, Gas B (2004) Electrophoresis 25:309–317
15. Zuskova I, Novotna A, Vcelakova K, Gas B (2006) J Chromatogr B 841:129–134
16. Barron D, Jimenez-Lozano E, Irles A, Barbosa J (2000) J Chromatogr 871:381–389
17. Barron D, Jimenez-Lozano E, Barbosa J (2000) J Chromatogr 871:395–406
18. Ishihama Y, Nakamura M, Miwa T, Kajima T, Asakawa N (2002) J Pharm Sci 91:933–942
19. Miller JM, Blackburn AC, Shi Y, Melzak AJ, Ando HY (2002) Electrophoresis 23:2833–2841
20. Wan H, Holmen A, Nagard M, Lindberg W (2002) J Chromatogr 979:369–377
21. Szakacs Z (2006) Electrophoresis 27:3399–3409
22. Zhou C, Jin Y, Kenseth JR, Stella M, Wehmeyer KR, Heineman WR (2005) J Pharm Sci 94:576–589
23. Geiser L, Henchoz Y, Galland A, Carrupt PA, Veuthey JL (2005) J Sep Sci 28:2374–2380
24. Davies CW (1938) J Chem Soc 2093–2098
25. Nancollas GH, Tomson MB (1982) Pure Appl Chem 54:2675–2692
26. Onsager LL (1926) Physik Z 27:388–392
27. Onsager LL (1927) Physik Z 28:277–298
28. Li D, Fu S, Lucy CA (1999) Anal Chem 71:687–699
29. Xu X, Kok WTh, Poppe H (1996) J Chormatogr 742:211–227
30. Beckers JL, Bocek P (2003) Electrophoresis 24:518–535
31. Avdeef A (2003) Absorption and drug development. Wiley & Sons, Hoboken
32. Dawson RMC, Elliott DC, Elliott WH, Jones KM (1986) Data for biochemical research. Oxford Science, New York
33. Passing H, Bablok W (1983) J Clin Chem Clin Biochem 21:709–720
34. Passing H, Bablok W (1988) J Clin Chem Clin Biochem 26:783–790
35. Wan H, Holmen AG, Wang Y, Lindberg W, Englund M, Nagard MB, Thompson RA (2003) Rapid Commun Mass Spectrom 17:2639–2648